Current Biology 20, 1296–1303, July 27, 2010 ©2010 Elsevier Ltd All rights reserved DOI 10.1016/j.cub.2010.05.061

Report

LGL Can Partition the Cortex of One-Cell *Caenorhabditis elegans* Embryos into Two Domains

Carsten Hoege,[1,*] Alexandru-Tudor Constantinescu,[1,2] Anne Schwager,[1] Nathan W. Goehring,[1] Prateek Kumar,[1] and Anthony A. Hyman[1]
[1]Max Planck Institute of Molecular Cell Biology and Genetics (MPI-CBG), Pfotenhauerstrasse 108, 01307 Dresden, Germany

Summary

Many metazoan cell types are polarized by asymmetric partitioning of the conserved PAR (PAR-3/PAR-6/PKC-3) complex [1–5]. Cortical domains containing this PAR complex are counterbalanced by opposing domains of varying composition [6–10]. The tumor-suppressor protein LGL [11, 12] facilitates asymmetric localization of cell fate determinants, in part through modulating the activity of the PAR complex [13, 14]. However, the mechanisms by which LGL acts to maintain a cortical domain remain unclear. Here we identify *Caenorhabditis elegans* LGL in a biochemical complex with PAR proteins, which localize to the anterior cortex. But LGL itself localizes to the posterior cortex. We show that increasing the amounts of LGL can restrict localization of the PAR complex to an anterior cortical domain, even in the absence of PAR-2. Importantly, LGL must be phosphorylated on conserved residues to exert this function. LGL and the PAR complex can maintain two cortical domains that are sufficient to partition cell fate determinants. Our data suggest a mechanism of "mutual elimination" in which an LGL phosphorylation cycle regulates association of the PAR complex with the cortex: binding of LGL to the PAR complex at the interface of the two domains stimulates its phosphorylation by PKC-3, and the whole complex leaves the cortex.

Results and Discussion

Identification of *Caenorhabditis elegans* LGL

We purified protein complexes of the conserved protein PAR-6 by immunoprecipitation from synchronized gravid hermaphrodites and identified PAR-6 coprecipitating bands on gels after electrophoresis (Figure 1A). The identity of specifically copurifying species was analyzed by mass spectrometry [15]. The most abundant specific protein band was at 80 kDa and contained the *Caenorhabditis elegans* atypical protein kinase C (PKC-3); a band at about 120 kDa contained the protein F56F10.4. The closest homologs to F56F10.4 by BLAST are LGL family members, and, indeed, F56F10.4 shows characteristic phosphorylation sites [16, 17] conserved among LGL species (see Figure S1D available online). Therefore, we named *f56f10.4* now *lgl-1* and refer to it hereafter as *lgl*. We confirmed that F56F10.4 interacts with PAR-6 and PKC-3 in embryos by expressing GFP-F56F10.4 under the control of the *pie-1* promoter and purifying GFP-F56F10.4 protein complexes containing PAR-6 and PKC-3 by immunoprecipitation (Figure 1B).

*Correspondence: hoege@mpi-cbg.de
[2]Present address: Spezialklinik Neukirchen, Krankenhausstrasse 9, 93453 Neukirchen, Germany

LGL Localizes Asymmetrically to the Posterior Cortex in *C. elegans* One-Cell Embryos

We investigated LGL localization by expressing genomic *lgl* (Figures S1A and S1B) fused to *gfp* under the control of the *pie-1* promoter. After polarity onset, GFP-LGL becomes enriched at the posterior cortex and segregates after division to the posterior P_1 cell (Figure 1D). This localization is similar to GFP-PAR-2 [8], and, indeed, both proteins colocalize on the posterior cortex domain in lines expressing both mcherry-PAR-2 and GFP-LGL (Figure 1E). We confirmed the posterior localization by using antibodies raised against LGL (see Experimental Procedures) in immunofluorescence experiments. This showed that LGL localizes to the posterior cortex (Figure 1F), similar to PAR-1 and PAR-2 localization [18, 19]. Therefore, we conclude that LGL is part of the posterior cortex domain.

Genetic Interaction of *lgl* with *par-2* Alleles

We isolated *lgl-1* alleles (Figures S1A–S1C and S1E) and found that *lgl* is not essential for survival and showed no phenotypic abnormalities in the first cell division. The extent of the PAR-6 domain on the cell cortex and nonmuscle myosin organization at the cortex was indistinguishable from wild-type (WT) (Figures S2B, S2D, and S2E). Epithelial integrity at later stages of development also appeared to be unaffected. Adherens junctions and GFP-PAR-6, which mark the apical side of cells in the developing intestine [20, 21], localize normally (Figure S2A). Because *lgl* is essential for cell polarity in other systems [16, 22–25] and LGL can regulate the subunit composition of the PAR complex [14], we looked for genetic interaction between LGL and the PAR proteins. We fed wild-type *N2* or *lgl-1(dd21)* worms with *par-2(RNAi)* feeding bacteria for different times and scored the appearance of *par-2*-specific symmetric first divisions of the embryo. Surprisingly, we found that *lgl-1(dd21)* mutants are hypersensitive to *par-2(RNAi)* (Figures 2A and 2B). We further investigated this interaction using *par-2* mutants. Although *par-2ts(it5)* mutants treated with a control RNA (i.e., *klp-1(RNAi)*) showed about 15% embryonic lethality at the semipermissive temperature (20°C), lethality increased to 87% in combination with *lgl(RNAi)* (Figures 2C and 2D). Similar lethality was observed when we crossed the *lgl-1* alleles into the *par-2ts(it5)* background. Only about 5% of the *par-2ts(it5)* embryos failed to hatch at the permissive temperature (16°C), but this fraction increased to 97% in the double mutant, indicating that LGL function is essential in the *par-2ts(it5)* background (Figures 2E and 2F). Because LGL has been implicated in negative regulation of nonmuscle myosin activity in *Drosophila* [24, 26–28], we looked for genetic interaction between *lgl* and *nmy-2* mutants. We observed a slight increase in embryo lethality in double mutants, although this was not statistically significant (Figure S2C). In addition, cortex contractility appears to be normal in *lgl-1(dd22)* mutants (Figure S2B). Therefore, LGL does not seem to directly affect contractility of the cell cortex and instead acts with PAR proteins.

LGL Activity Compensates for PAR-2 Depletion

To understand how LGL could act together with PAR proteins, we looked at whether LGL localization depends on PAR

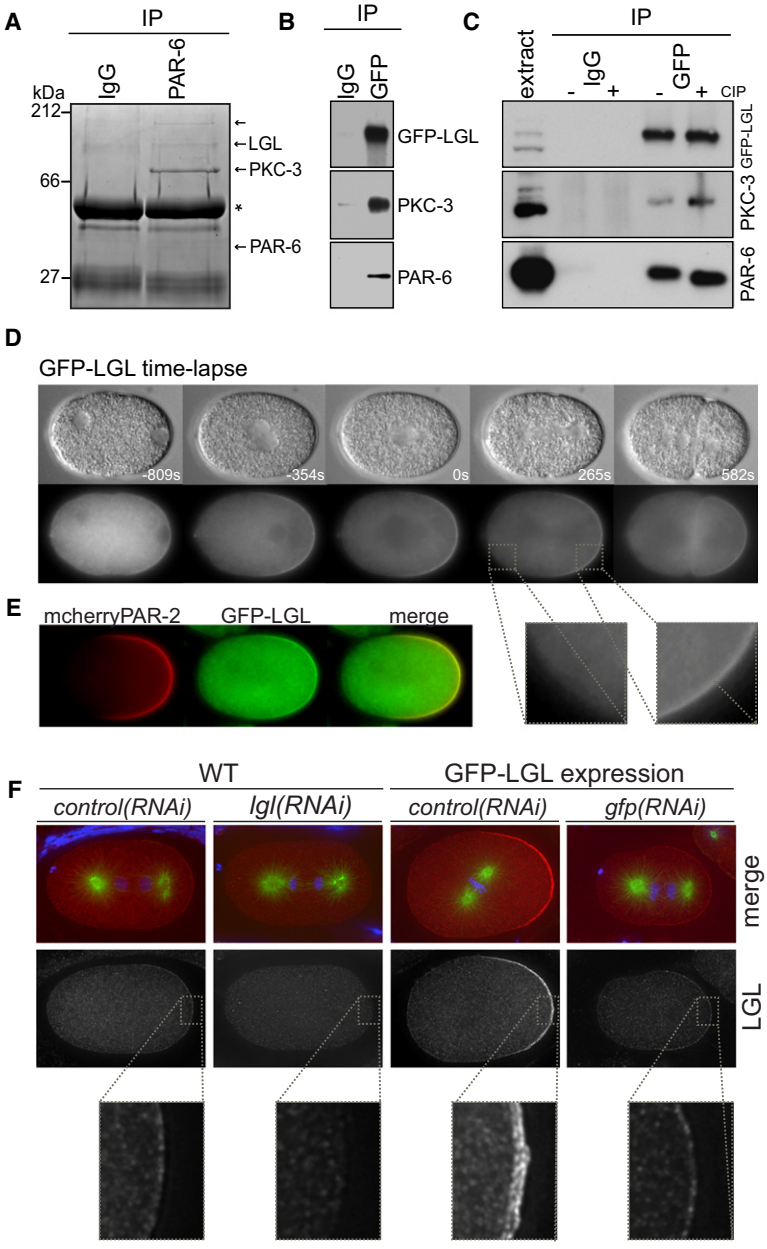

Figure 1. LGL Interacts with Anterior PAR Complex Proteins but Localizes to the Posterior Cortex

(A) LGL and PKC-3 interact with *Caenorhabditis elegans* PAR-6. Anti-PAR-6 immunoprecipitations were made from wild-type *C. elegans* worms. Proteins were stained with Coomassie, and specific bands were excised and identified by matrix-assisted laser desorption/ionization time-of-flight mass spectrometry [15]. PAR-6 (36 kDa) stains only weakly by Coomassie. The 80 kDa band contained PKC-3, the 120 kDa band contained the protein of *F56F10.4/lgl*, and a third band at 180 kDa contained the protein of *W07E11.1*. * denotes IgG bands.

(B) GFP-LGL interacts with PKC-3 and PAR-6 in *C. elegans* embryos. Immunoblots were made from anti-GFP immunoprecipitation from GFP-LGL-expressing embryos.

(C) The LGL complex is sensitive to phosphatase treatment. Anti-GFP immunoprecipitations from GFP-LGL-expressing embryos were left untreated (−) or treated (+) with calf intestine phosphatase (CIP). Proteins were detected by immunoblot.

(D) GFP-LGL localizes to the posterior cortex after polarity onset. Images are from time-lapse recording. Times are relative to nuclear envelope breakdown (0 s). Top row: differential interference contrast images; bottom row: GFP-LGL fluorescence. Note the blow-up of the anterior and posterior cortex region.

(E) LGL colocalizes with PAR-2. mcherry-PAR-2 and GFP-LGL from a double fluorescent cell line colocalize on the posterior cortex of the one-cell embryo.

(F) Immunofluorescence of LGL in embryos treated with *control(RNAi)*, *lgl(RNAi)*, or GFP-LGL-expressing embryos, or GFP-LGL embryos silenced only for the transgene *gfp::lgl* by *gfp(RNAi)* (DNA, blue; microtubules, green; LGL, red). All images were taken with identical exposure conditions and processed identically. For quantifications, see Figure S1F.

proteins. After depletion by RNA interference (RNAi) of either *par-3* or *pkc-3*, GFP-LGL behaved like PAR-2 [18], localizing throughout the cortex, and the embryos divided symmetrically (Figure 3A). In *par-1(RNAi)* embryos, GFP-LGL localization is not notably affected, but these embryos showed a *par* phenotype and divided symmetrically. However, in *par-2(RNAi)* embryos, GFP-LGL localization is also not notably affected, but embryos divide asymmetrically like in WT embryos (Figure 3A). This is surprising because *par-2(RNAi)* leads to a loss of endogenous LGL localization and a uniform localization of anterior PAR proteins to the cell cortex in otherwise WT embryos (Figures S3A and S3A'). Furthermore, GFP-LGL localizes to the cell periphery of cells of the P lineage, and asymmetric divisions of the P lineage and GFP-LGL localization are not changed by *par-2(RNAi)* (Figure 3B). We eliminated the possibility that GFP-LGL expression is preventing depletion of PAR-2 by *par-2(RNAi)* using immunoblots and immunofluorescence (Figure 3C; Figures S3B and S3C). Therefore, we conclude that GFP-LGL expression is suppressing the phenotype of *par-2(RNAi)*.

To further verify that *par-2(RNAi)* rescue is indeed caused by transgenic GFP-LGL expression, we developed an assay in which we could specifically silence the transgene (for further details, see Experimental Procedures). We fed either wild-type or transgenic *gfp::lgl* worms an equal mix of *par-2/control(RNAi)* bacteria or *par-2/gfp(RNAi)* bacteria. *gfp(RNAi)* will deplete *gfp::lgl* but not endogenous *lgl*. Although we obtained high embryonic lethality for wild-type *N2* worms with both RNAi conditions as expected, we observed rescue of *par-2/control(RNAi)* for GFP-LGL-expressing worms (Figure 3D). However, when we silenced both *par-2* and the *gfp::lgl* transgene by *par-2/gfp(RNAi)*, we observed high embryonic lethality (Figure 3D), strongly arguing for suppression of the *par-2* phenotype by GFP-LGL expression. A clue to explain how GFP-LGL expression suppresses the *par-2 (RNAi)* phenotypes came from immunofluorescence experiments. They showed that LGL fluorescence intensities on the posterior cortex are about 3-fold increased in embryos additionally expressing *gfp::lgl* and that intensities could be diminished to wild-type LGL levels by specific silencing of *gfp::lgl* by *gfp(RNAi)* (Figure 1F; Figure S1F). This suggests that GFP-LGL is suppressing the *par-2(RNAi)* phenotype because it is moderately overexpressed compared to wild-type LGL.

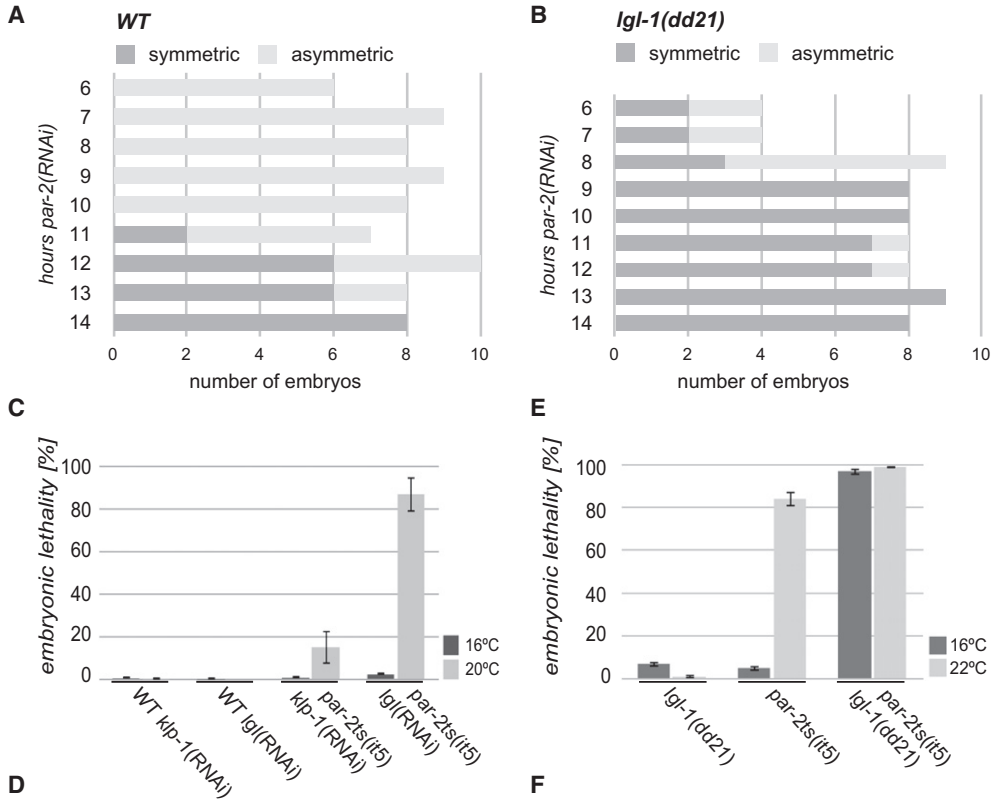

D

strain	emb. let. 16ºC	emb. let. 20ºC
WT klp-1(RNAi)	0.45%±0.13% (n=1797)	0.16%±0.11% (n=625)
WT lgl(RNAi)	0.16%±0.09% (n=1887)	0.00%±0.00% (n=543)
par-2ts(it5) klp-1(RNAi)	0.85%±0.54% (n=1117)	15.10%±7.95% (n=368)
par-2ts(it5) lgl(RNAi)	2.30%±1.05% (n=1071)	87.00%±8.33% (n=322)

F

strain	emb. let. 16ºC	emb. let. 22ºC
lgl-1(dd22)	1.7%±1.0% (n=578)	ND
lgl-1(dd21)	7.3%±1.6% (n=138)	0.7%±1.0%(n=141)
par-2ts(it5)	4.7%±1.6% (n=295)	84.0%±3.6%(n=154)
par-2ts(it5) lgl-1(dd21)	96.6%±1.9% (n=1455)	99.0%±0.5%(n=384)
par-2ts(it5) lgl-1(dd22)	100%±0.0% (n=308)	ND

Figure 2. Genetic Interaction of *lgl* and *par-2*

(A and B) *lgl* mutants are hypersensitive to *par-2* depletion. *N2* wild-type (WT) worms (A) or *lgl-1(dd21)* worms (B) were placed on *par-2(RNAi)* feeding plates for indicated times. Appearance of *par-2* phenotype (symmetric division) of one-cell embryos after each time point was scored by microscopy.
(C–F) Viability of *par-2ts(it5)* embryos is dependent on *lgl.*
(C and D) *lgl(RNAi)*, but not control *klp-1(RNAi)*, strongly increases embryo lethality in *par-2ts(it5)* mutants.
(E and F) *par-2ts lgl-1* embryos are lethal at the permissive temperature (16˚C). Error bars in (C)–(F) indicate standard error of the mean (SEM); n indicates total number of counted embryos.

LGL Activity Compensates for PAR-2 Depletion by Restoring Cell Polarity

We wanted to investigate whether embryo viability in GFP-LGL-expressing worms is restored by rescuing the asymmetric localization of the PAR complex or rather by some other bypass mechanism. Indeed, mcherry-PAR-6 was restricted to the cortex of the anterior AB cell in *par-2/control(RNAi)* embryos expressing GFP-LGL (Figures 3E and 3F). We confirmed this by immunofluorescence against endogenous PAR-6, which showed that PAR-6 fluorescence is restored to that seen in wild-type *N2* embryos (Figures 3G and 3H; Figure S3J). We then asked whether localization of other PAR complex proteins is restored as well. Neither PKC-3 nor PAR-3 localized to the P_1 cortex after *par-2/control(RNAi)* (Figures S3D–S3G). Importantly, as before, this exclusion was dependent on GFP-LGL expression, because RNAi of *gfp::lgl* by *gfp(RNAi)* abolished the asymmetric localization of the PAR complex (Figure 3H; Figures S3D–S3G). Thus, we conclude that LGL itself has cortex partitioning activity and can restrict localization of the PAR complex.

P granules are cytosolic cell fate determinants. Their formation and localization depends on the activity of PAR proteins that localize to the posterior cortex [18, 19, 29, 30]. To test whether LGL expression could compensate for P granule defects seen in *par-2*-depleted embryos, we analyzed the P granule component PGL-1. GFP-LGL expression restored the normal size and shape of P granules, which accumulated in the posterior half of the embryo in *par-2/control(RNAi)* embryos (Figure 3I). However, when *gfp::lgl* is silenced by RNAi, P granules mostly disintegrate (Figure 3J). Because formation of P granules also requires PAR-1 activity [19, 30], we reasoned that PAR-1 localization to the cortex might be restored by GFP-LGL expression. However, this is not the case, and only residual PAR-1 remains on the cortex (Figures S3H–S3I'). We conclude that LGL partitions not only the PAR complex on the cortex but also cell fate determinants in the cytosol.

LGL Activity Is Regulated by PKC-3-Dependent Phosphorylation

We have shown so far that when we silenced *par-3* or *pkc-3* by RNAi, GFP-LGL localization extended over the whole embryo cortex (Figure 3A). This means that a functional anterior PAR

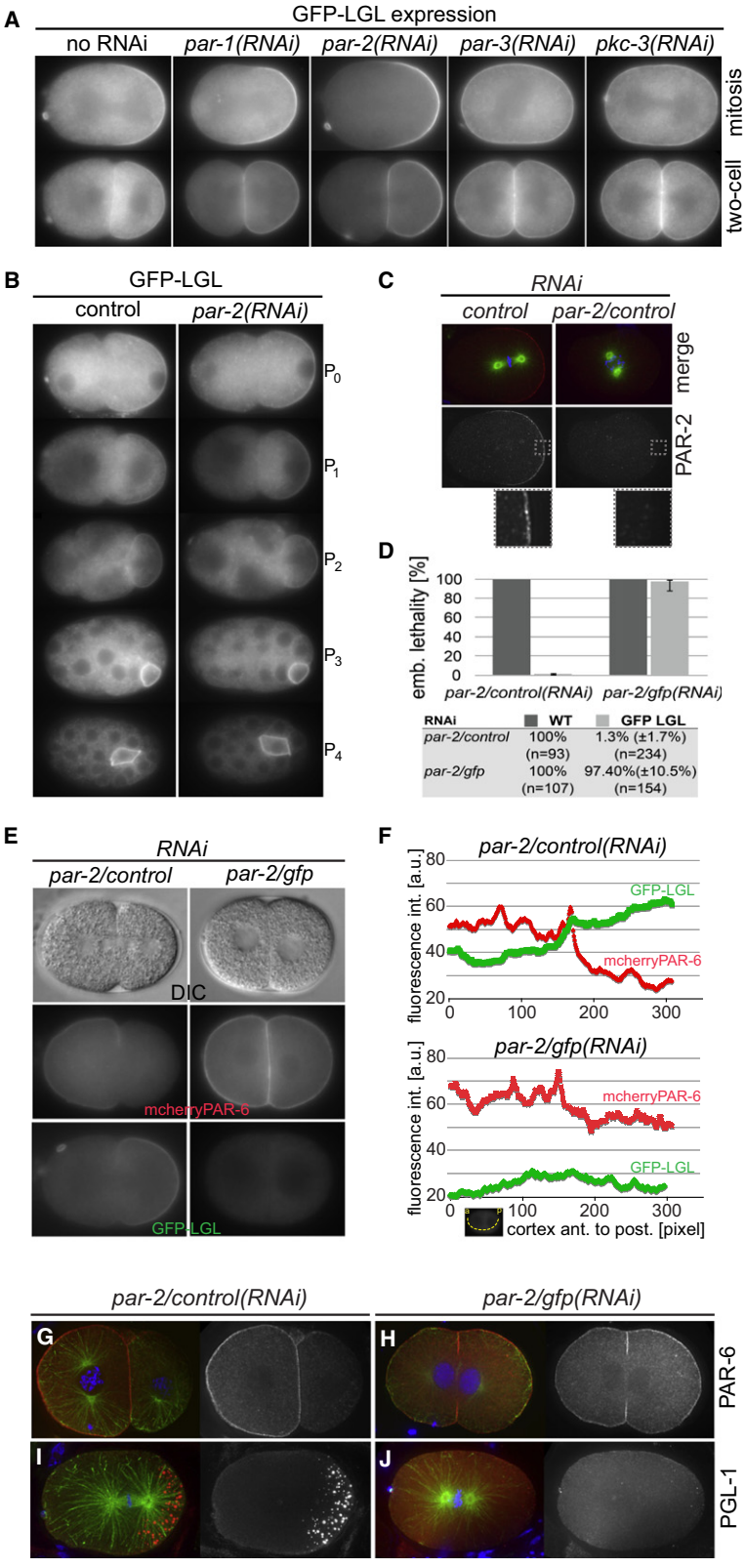

Figure 3. GFP-LGL Expression Compensates for Depletion of PAR-2 by Restoring Cell Polarity

(A) GFP-LGL localization depends on anterior PAR proteins. GFP-LGL localizes uniformly to the cortex in *par-3(RNAi)* and *pkc-3(RNAi)* embryos. Note that there is still asymmetric division in the *par-2(RNAi)* embryo.

(B) GFP-LGL localizes to the cell periphery of P lineage cells. Depletion of *par-2* by RNA interference (RNAi) does not lead to symmetric division of P lineage cells in GFP-LGL-expressing embryos, nor to loss of LGL localization (in 14 of 14 embryos).

(C) PAR-2 is efficiently depleted by RNAi in GFP-LGL-expressing embryos. Anti-PAR-2 immunofluorescence was made from *par-2/control(RNAi)*-treated embryos (DNA, blue; microtubules, green; PAR-2, red). For quantification of PAR-2 cortex fluorescence, see Figure S3C.

(D) Embryonic lethality of *par-2(RNAi)* is rescued by GFP-LGL expression (*par-2/control(RNAi)*). Silencing of *par-2* and the transgene *gfp::lgl* by *(par-2/gfpRNAi)* leads to high embryo lethality. Mean ± SEM, n indicates total number of counted embryos.

(E and F) mcherryPAR-6 localization is restricted to the anterior by GFP-LGL expression in *par-2*-depleted embryos. Of *par-2/control(RNAi)* embryos, 5 of 5 showed *par-2* phenotype rescue; 7 of 7 *par-2/gfp(RNAi)* embryos showed a *par-2* phenotype.

(F) Quantification of anterior-to-posterior cortex fluorescence of mcherryPAR-6 and GFP-LGL (from images in E).

(G and H) PAR-6 localization is restricted to the anterior AB cell when *gfp::lgl* is expressed (in 10 of 10 embryos; *par-2/control(RNAi)*) but is not restricted if *gfp::lgl* is silenced (in 6 of 7 embryos; *par-2/gfp(RNAi)*).

(I and J) GFP-LGL expression restores posterior localization of P granules in *par-2*-depleted embryos (8 of 8 embryos), but depletion of *gfp::lgl* leads to loss of P granules (7 of 7 embryos).

complex is required to restrict localization of LGL to the posterior, just as it is for PAR-2 [8, 18]. How does the anterior PAR complex restrict LGL to the posterior? It is known that LGL is phosphorylated by aPKC on conserved serine residues [10, 16, 17]. To test whether LGL restriction to the posterior is regulated by PKC-3-dependent phosphorylation, we expressed a version of GFP-LGL in which we mutated all three conserved sites to alanines. The localization of the GFP-LGL AAA mutant protein is not restricted to the posterior cortex anymore but localizes uniformly to both domains throughout the first cell division (Figure 4A) and is not restricted to the P lineage (data not shown). We also looked at phosphomimetic LGL [10] by exchanging the three conserved serine/threonines with glutamates (GFP-LGL EEE). Strikingly, GFP-LGL EEE was unable to associate with the cortex (Figure 4A), even in the absence of a functional PAR complex (Figures S4F–S4H). Therefore, the association of LGL with the cortex appears to take place only if the protein is not phosphorylated on the conserved sites.

We next asked whether the uniform localization of GFP-LGL AAA is sufficient to remove the anterior PAR complex from the cortex by looking at the distribution of PAR-3 and PAR-6 in *par-2(RNAi)* embryos expressing GFP-LGL AAA. Interestingly, although GFP-LGL AAA localized uniformly to the cortex in these embryos (Figures S4A and S4B), PAR-3 and PAR-6 still localize to the cortex, and their localization is not restricted to the anterior (Figures S4C and S4D). Confirming this result, GFP-LGL AAA expression could not rescue the lethality of *par-2(RNAi)* (Figure 4B; Figure S4E). We conclude that LGL must be phosphorylated to

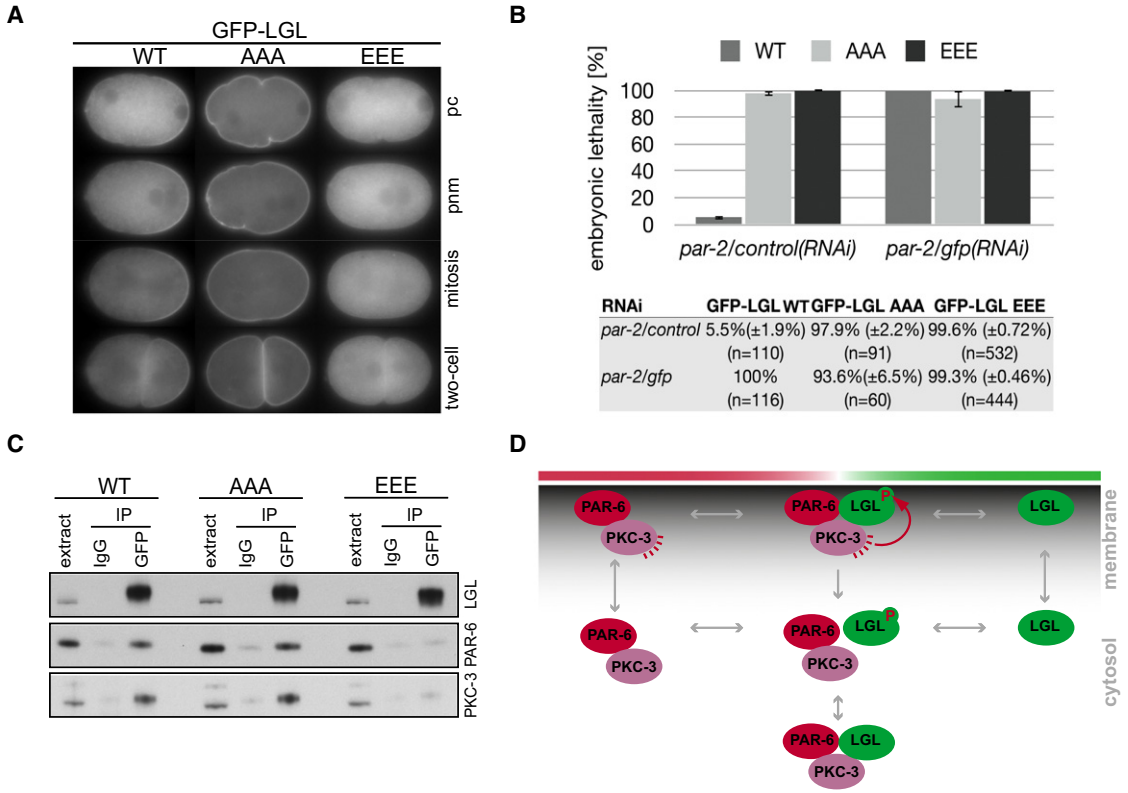

Figure 4. LGL Localization to the Cell Cortex and Interaction with PAR Complex Proteins Are Regulated by Phosphorylation

(A) LGL phosphorylation sites are required for cell-cycle-specific localization. S661, S665, and T669 are unchanged (WT, left), changed to alanines (AAA, middle), or changed to glutamates (EEE, right) to mimic phosphorylation. Staging: pc, pseudocleavage, pnm, pronuclear meeting.

(B) LGL phosphorylation sites are required to rescue *par-2* embryonic lethality. Mean ± SEM, n indicates number of total counted embryos.

(C) GFP-LGL AAA interacts with PAR-6 and PKC-3 as the GFP-LGL WT protein. GFP-LGL EEE associates only weakly with PKC-3 and PAR-6.

(D) A model for maintenance of two cortical domains by mutual elimination in *C. elegans* embryos. LGL and the PAR complex diffuse on the membrane and turn over at the domain boundary by mutual elimination, which includes an LGL phosphorylation cycle that inactivates both LGL and the PAR complex. Association of LGL to PAR-6/PKC-3 forms the LGL complex. PKC-3 activity leads to LGL phosphorylation, and the LGL complex drops off the cortex because phosphorylated LGL cannot associate with the membrane anymore.

deplete PAR-3 and PAR-6 from the posterior cortex and to restore embryo viability. However, because the GFP-LGL EEE phosphomimetic protein localizes to the cytosol and cannot rescue lethality of *par-2(RNAi)* embryos (Figure 4B), phosphorylated LGL is also not sufficient to restore embryo viability. Therefore, we conclude that cortex partitioning activity of LGL requires phosphorylation changes in LGL.

LGL Phosphorylation Modifies the Association with PAR Complex Proteins

To investigate whether phosphorylation of LGL affects the binding of complex partners, we purified either GFP-LGL WT, GFP-LGL AAA, or GFP-LGL EEE protein complexes from early embryos by immunoprecipitations. Importantly, the WT and the unphosphorylated AAA form both bind well to PAR-6 and PKC-3 (Figure 4C). However, the association of the phosphomimetic EEE form with PKC-3 and PAR-6 is much weaker (Figure 4C). We also noted in our initial immunoprecipitation experiments that treatment of the immunopurified LGL complex with phosphatase increased association of PKC-3 with the complex (Figure 1C). Therefore, we conclude that phosphorylation not only changes the localization of LGL but also affects the composition of the LGL complex.

Model and Conclusions

Although genetic results have indicated that the formation of cortical domains of PAR proteins requires mutual inhibition [6, 9, 18, 31–33], we do not have a good understanding of the enzymology of the interactions between proteins of the two cortex domains. In this work we have now identified the LGL homolog in *C. elegans*, shown that LGL is sufficient to partition the cortex, and demonstrated that this activity is directly linked to its phosphorylation. An explanation of how LGL activity is involved in polarity of the first-cell *C. elegans* embryo must explain the seemingly contradictory results that LGL is found associated with the anterior PAR complex proteins PAR-6 and PKC-3 by immunoprecipitation, but that, by light microscopy, LGL localizes to the opposite posterior cortex. To reconcile these observations with the activities of the GFP-LGL AAA and EEE mutants, we propose the following model (see Figure 4D): LGL on the cortex binds the PAR complex most likely at the boundary between the anterior PAR domain and the posterior LGL domain, forming the PAR-6/PKC-3/LGL complex. PKC-3 will then phosphorylate LGL, and the whole complex will drop off the cortex. This model can be thought of as "mutual elimination," in which interaction between LGL and the anterior PAR complex at the boundary between the two complexes causes both to leave the cortex. PAR proteins

appear to move on the cortex by lateral diffusion [34] (Goehring et al., personal communication). LGL might show similar diffusion, and mutual elimination between LGL and the anterior PAR complex at domain boundaries could, in part, explain maintenance of two domains on the cell cortex.

Different strategies seem to have evolved in cells to maintain two cortex domains on the cell membrane, but all might include direct inhibition of the PAR complex by an opposing activity. Because LGL is conserved in metazoans [35], future work needs to address the contribution of LGL and other opposing activities on the PAR complex in different cell types.

Previous work in *Drosophila* has shown that Aurora A phosphorylation of PAR-6 stimulates phosphorylation of LGL by aPKC, which activates the PAR complex [14]. This work suggested that LGL acts as a buffer, possibly in the cytoplasm where it holds the PAR complex inactive until phosphorylated by Aurora A. In *C. elegans*, Aurora A activity is likely high throughout the first cell cycle [36] and could maintain an active PAR complex by releasing sufficient LGL. More generally, the rate of LGL dissociation from the LGL/PAR-6/aPKC complex may determine the available pool of PAR complexes for cell polarity in the one-cell embryo. Therefore, the combination of these two models can explain the function of LGL. On the one hand, it acts as a buffer [14]. On the other hand, LGL acts through mutual elimination to remove the conserved PAR complex from the cortex.

Experimental Procedures

C. elegans Worm Lines and Cloning

All *C. elegans* strains were grown on nematode growth medium (NGM) plates and handled as described [37]. *lgl* was polymerase chain reaction amplified from genomic *N2* DNA with primers 5′TTAACTAGTGGAATGAGC AGCATCTTACGATTT3′ and 5′TATAGGCCTCTATGACTTGTGCGTACTGC3′ and subcloned into pGEM-T (Promega). The sequence was verified, and a SpeI and StuI fragment was cloned into pTH314 (*gfp::lgl* fusion under control of *pie-1* promoter and terminator). Transgenic lines expressing GFP-LGL (TH270), GFP-LGL AAA (TH271), or GFP-LGL EEE (TH272) were made from genomic *lgl* by particle bombardment of *unc-119(ed3)* worms [38] and were maintained at 25°C. Other worm lines were mcherry-PAR-2 (TH209; [29]), mcherry-PAR-6 [39], and NMY-2-GFP [40]. Double fluorescent lines were made by crossing the relevant single lines. *lgl* gene structure was derived from first-strand cDNA made from *N2* polyA RNA. Site-directed mutagenesis (QuikChange, Stratagene) and DNA sequencing were used to introduce and verify mutations in *lgl*.

Identification of *lgl* Alleles by Deletion Screening

lgl-1(dd21) (TH131) and *lgl-1(dd22)* (TH132) were generated by ethyl methanesulfonate-mediated mutagenesis [41]. The mutant alleles were isolated with the nested primer pairs 5′GATGTCAACCAGAGACTGGCCG3′ and 5′AC TCGAGTTTAGTGCCATTACGTC3′ and 5′ATCAACGAGCTTCTTACCGACA AG3′ and 5′GAAACTTAACCACTTCTCAGCGCC3′ and backcrossed seven times to *N2*. The deletions were verified by amplification and sequencing of *lgl-1(dd21)* and *lgl-1(dd22)* cDNA and by western blotting with anti-LGL antibody.

Gene Silencing by RNAi and Embryonic Lethality Assays

Gene silencing by RNAi was done by feeding [42, 43]. Briefly, overnight cultures grown in LB Amp Tet were diluted to fresh LB Amp, grown to log phase, and induced with 0.2 mM IPTG at 30°C for 2 hr and plated onto fresh NGM feeding plates for further 1 day growth. L4 or young adults were placed on feeding plates for 24–28 hr at 25°C for RNAi experiments. For feeding assays with two genes, bacterial cultures of similar optical densities were mixed 1:1. Feeding assays for *par-2/control(RNAi)* and *par-2/gfp(RNAi)* in *gfp::lgl*-expressing worms were done in parallel on 3–6 plates, using identical conditions, and embryonic lethality was assayed as ratio of dead embryos to total number (n) of embryos (in Figure 3D; Figures S3D–S3J; Figure 4B; Figure S4E). A drop in penetrance of *par-2(RNAi)* compared to *par-2/control(RNAi)* or *par-2/gfp(RNAi)*, respectively, was not observed. For *gfp(RNAi)*, a *gfp* cDNA fragment was cloned into L4440. *control(RNAi)* was done with empty L4440 plasmid. Three independent transgenic *gfp::lgl* lines rescued embryonic lethality of *par-2(RNAi).* For assaying synthetic embryonic lethality by RNAi, *lgl(RNAi)* or *klp-1(RNAi)* (as a control) was done by feeding for 3 days at 16°C and 1 day at 20°C or 4 days at 16°C in wild-type *N2* or *par-2ts(it5)* animals. Animals were allowed to lay eggs for 4–6 hr; eggs were counted and embryonic lethality was scored 24 hr later. For assaying synthetic lethality of double mutants, *lgl-1(dd21)* or *lgl-1(dd22)* animals were crossed to the relevant lines and screened for homozygous offspring. *par-2ts(it5)* worms (KK114) contain an additional *daf-7(e1372)* mutation that does not influence lethality with *lgl.* For *nmy-2 lgl-1(dd21)* lethality assays, *nmy-2(ne1490)ts* (WM180) worms were crossed into the *lgl* background and scored for embryonic lethality at indicated temperatures.

Antibodies

A set of 36 LGL GST-fusion fragments was cloned (USER system, New England Biolabs) and screened for solubility by an enzyme-linked immunosorbent assay. Three soluble fragments with high expression were purified from protein gels, used for injection of rabbits (Charles River Laboratories, France), and tested in worms. IgG from two sera were further used and affinity purified by corresponding MBP-fusion protein columns (primers of fragments used were forward 5′ggggagcuTTAATATGCACAAAATGCGA GAT3′, reverse 5′ggggaacuTATTTGATAACCCGCATTGTAC3′ and forward 5′ggggagcuCGCACTTCATTGGAGTTTGAC3′, reverse 5′ggggaacuTCGCTT TGGACTTGTCTCATG3′).

Antibodies against PAR-1, PAR-2, and PAR-3 were made from insoluble 6×Histidine-tagged fusions, purified under denaturing conditions (according to QIAGEN protocols), and used for injection of rabbits (Charles River Laboratories, France). PAR-6 antibodies were made from an N-terminal GST-PAR-6 fragment in rabbits and were affinity purified against PAR-6. IgG from PAR-1 and PAR-2 serum was affinity purified on corresponding GST-fusion columns and stored in phosphate-buffered saline (PBS) with 50% glycerol at −20°C. Anti-PGL-1 antibody (guinea pig) was a gift from Christian Eckmann (MPI-CBG, Dresden); anti-PKC-3 antibody for biochemistry was a gift from Monica Gotta (Geneva); for PKC-3 immunofluorescence, we used PKCzeta (C20, Santa Cruz Biotechnology); and MH27 (Jam-1) was received from the Developmental Studies Hybridoma Bank (DSHB).

Immunoprecipitations and Western Blots

For large-scale anti-PAR-6 immunoprecipitation (Figure 1A), 1×10^7 dauer larvae from wild-type *N2* were released on 15 egg plates and grown for 35 hr at 24.5°C. Adult worms containing 1 to 8 cell embryos were harvested and washed twice with H100 buffer (50 mM HEPES, pH 7.5, 100 mM KCl, 1 mM $MgCl_2$, 1 mM EGTA, 10% glycerol) and frozen in liquid nitrogen. An equal volume of H100 buffer (with 0.05% NP-40 and protease inhibitors) was added to pellets, and worms were lysed on ice by sonication (six cycles of 15 s). Lysates were clarified by 100,000 × g centrifugation for 30 min and incubated with 12 μg anti-PAR-6 IgGs for 45 min at 4°C. Immunocomplexes were collected by protein A agarose (General Electric), washed five times with lysis buffer, and eluted with 1 M glycine (pH 2.3), neutralized and supplemented with Laemmli buffer. Proteins were separated on SDS-PAGE gels (Hoefer). Coomassie-stained bands were in gel digested with trypsin, and proteins were identified by matrix-assisted laser desorption/ionization time-of-flight mass spectrometric peptide mapping [15]. Worms for immunoprecipitation from early embryos (Figures 1B and 1C; Figure 4C) were grown on peptone plates made with 3.6% agar and seeded with C600 bacteria. Embryos were purified by bleaching and hatched overnight in S-Basal complete, and the L1 larvae were seeded with a density of about 1×10^5 per 15 cm peptone (seeded with C600 bacteria) plate and grown at 25°C. Synchronized, adult worms were harvested before embryos were laid, and embryos were purified by bleaching, frozen in liquid N_2, and stored at −80°C. Embryo pellets (500 μg) were taken up in 500 μl volume 2×H100 buffer (100 mM HEPES at pH 7.5, 200 mM KCl, 2 mM $MgCl_2$, 2 mM EGTA, 20% glycerol, protease and phosphatase inhibitors), lysed on ice by 0.5 s sonication pulses for a total of 20 s, supplemented with 0.2% final Triton X-100 for 20 min on ice, and centrifuged for 1 hr at 230,000 × g in a TLA120.2 rotor. Supernatants were filtered (Ultrafree MC Millipore 0.45 μm) and incubated with goat anti-GFP IgG (protein expression facility, MPI-CBG) coupled to magnetic protein G beads (Invitrogen). Beads were washed four times with 1×H100 with 0.2% Triton X-100, once with 1×H100, 300 mM KCl with 0.2% Triton X-100, and once with H100 buffer and eluted with 50 μl 1% SDS. For phosphatase treatment (Figure 1C), the washed immunocomplexes were incubated for 20 min at 37°C with or without phosphatase (40 units calf intestine phosphatase, New England Biolabs). For immunoblots, protein extracts were diluted with sample buffer, run on gels as above,

blotted, and detected on polyvinylidene fluoride membranes (Millipore) by enhanced chemiluminescence (ECL, General Electric).

Microscopy

Live imaging of fluorescent worm lines was either on a Zeiss Axioplan II Widefield microscope with a Zeiss 63× 1.4 Apochromat lens and a Hamamatsu Orca ER 12-bit camera as described [39] or on a Zeiss Axio Imager Z1 microscope body (with a Apochromat, 63× and 1.4 lens), equipped with a Yokagawa spinning disc head, a Melles Griot 488 nm 43 series argon ion laser, and a Hamamatsu Orca ER 12-bit camera, and images were processed with ImageJ (http://rsb.info.nih.gov/ij/). For immunofluorescence, embryos were freeze cracked in liquid N_2, fixed for 20 min in −20°C methanol, rehydrated in PBS with 0.05% Tween-20 (PBS-T) and stained with antibodies overnight, washed with PBS-T, and probed with secondary antibodies (Alexa Dyes, Molecular Probes) and fluorescein isothiocyanate-conjugated anti-tubulin dm1α (Sigma). Images were taken on a DeltaVision RT imaging system (Applied Precision, LLC; IX70 Olympus) equipped with a charge-coupled device camera (CoolSNAP HQ; Roper Scientific) in 0.2 μm serial Z sections using an Olympus 100× 1.40 NA UPlanSApo. Image stacks were deconvolved using Softworx (Applied Precision, LLC) and processed in ImageJ. Images were maximum-intensity projected (all planes for microtubules and DNA; 10 midplane images for cortex proteins). All images of embryos show anterior on the left and posterior on the right.

Image Quantifications

Average fluorescence intensities from immunofluorescence pictures were measured from deconvolved and projected images (10 planes of 0.2 μm distance) by cortical 5-pixel-wide segmented lines spanning 0%–25% (anterior) or 75%–100% (posterior) of embryo length. Average cortex fluorescence intensities were normalized to background. Fluorescence intensities from live embryos were measured from a cortical 5-pixel-wide segmented line spanning 0%–100% of embryo length (cortex position anterior to posterior in pixel). All images for quantification were exposed and processed identically and made from slides prepared in parallel experiments. PAR-6 domain and boundary shape (Figures S2D and S2E) was extracted from 20-pixel-wide lines (spinning disk images from 6 frames, 20 s intervals). The sum of the three brightest pixels corresponding to an approximately 600 nm thick region spanning the membrane was taken at each point to generate a fluorescence profile around the entire embryo, and the absolute intensity was normalized to the mean fluorescence of the entire profile. The edges of the domain were fit using error functions (erf), with the center of each erf taken as the domain edge. Domain size is taken as the distance between these two edges and was normalized to the total length of the profile. To generate the average shape of the boundary profiles, we aligned individual boundary gradients by the domain edge, as defined by the center of the corresponding erf, and averaged them. Distance is absolute.

Supplemental Information

Supplemental Information includes four figures and can be found with this article online at doi:10.1016/j.cub.2010.05.061.

Acknowledgments

We would like to thank Bianca Habermann for help with identifying the *Drosophila* homolog of *F56F10.4*, Jan Havlis and Andrei Shevchenko for mass spectrometry, Andrei Pozniakovsky and Susanne Ernst for help with cloning and bombardment of transgenic constructs, Christian Eckmann and Andrea Zinke for help in setting up the deletion screen, Mike Tipsword for identifying soluble LGL fragments, and Monica Gotta for reagents. Some strains and antibodies were provided by the Caenorhabditis Genetics Center and the Developmental Studies Hybridoma Bank, respectively. We further thank Suzanne Eaton, Stefan Jentsch, Jens Roeper, and Elisabeth Knust for discussions and comments on the manuscript.

Received: February 4, 2010
Revised: May 12, 2010
Accepted: May 18, 2010
Published online: June 24, 2010

References

1. Cowan, C.R., and Hyman, A.A. (2007). Acto-myosin reorganization and PAR polarity in C. elegans. Development *134*, 1035–1043.
2. Goldstein, B., and Macara, I.G. (2007). The PAR proteins: Fundamental players in animal cell polarization. Dev. Cell *13*, 609–622.
3. Gönczy, P. (2008). Mechanisms of asymmetric cell division: Flies and worms pave the way. Nat. Rev. Mol. Cell Biol. *9*, 355–366.
4. Macara, I.G., and Mili, S. (2008). Polarity and differential inheritance—universal attributes of life? Cell *135*, 801–812.
5. Neumüller, R.A., and Knoblich, J.A. (2009). Dividing cellular asymmetry: Asymmetric cell division and its implications for stem cells and cancer. Genes Dev. *23*, 2675–2699.
6. Benton, R., and St Johnston, D. (2003). Drosophila PAR-1 and 14-3-3 inhibit Bazooka/PAR-3 to establish complementary cortical domains in polarized cells. Cell *115*, 691–704.
7. Böhm, H., Brinkmann, V., Drab, M., Henske, A., and Kurzchalia, T.V. (1997). Mammalian homologues of C. elegans PAR-1 are asymmetrically localized in epithelial cells and may influence their polarity. Curr. Biol. *7*, 603–606.
8. Cuenca, A.A., Schetter, A., Aceto, D., Kemphues, K., and Seydoux, G. (2003). Polarization of the C. elegans zygote proceeds via distinct establishmentand maintenance phases. Development *130*, 1255–1265.
9. Rolls, M.M., Albertson, R., Shih, H.-P., Lee, C.-Y., and Doe, C.Q. (2003). Drosophila aPKC regulates cell polarity and cell proliferation in neuroblasts and epithelia. J. Cell Biol. *163*, 1089–1098.
10. Yamanaka, T., Horikoshi, Y., Sugiyama, Y., Ishiyama, C., Suzuki, A., Hirose, T., Iwamatsu, A., Shinohara, A., and Ohno, S. (2003). Mammalian Lgl forms a protein complex with PAR-6 and aPKC independently of PAR-3 to regulate epithelial cell polarity. Curr. Biol. *13*, 734–743.
11. Gateff, E. (1978). Malignant neoplasms of genetic origin in Drosophila melanogaster. Science *200*, 1448–1459.
12. Hadorn, E. (1937). An accelerating effect of normal "ring-glands" on puparium-formation in lethal larvae of Drosophila melanogaster. Proc. Natl. Acad. Sci. USA *23*, 478–484.
13. Atwood, S.X., and Prehoda, K.E. (2009). aPKC phosphorylates Miranda to polarize fate determinants during neuroblast asymmetric cell division. Curr. Biol. *19*, 723–729.
14. Wirtz-Peitz, F., Nishimura, T., and Knoblich, J.A. (2008). Linking cell cycle to asymmetric division: Aurora-A phosphorylates the Par complex to regulate Numb localization. Cell *135*, 161–173.
15. Havlis, J., Thomas, H., Sebela, M., and Shevchenko, A. (2003). Fast-response proteomics by accelerated in-gel digestion of proteins. Anal. Chem. *75*, 1300–1306.
16. Betschinger, J., Mechtler, K., and Knoblich, J.A. (2003). The Par complex directs asymmetric cell division by phosphorylating the cytoskeletal protein Lgl. Nature *422*, 326–330.
17. Kalmes, A., Merdes, G., Neumann, B., Strand, D., and Mechler, B.M. (1996). A serine-kinase associated with the p127-l(2)gl tumour suppressor of Drosophila may regulate the binding of p127 to non-muscle myosin II heavy chain and the attachment of p127 to the plasma membrane. J. Cell Sci. *109*, 1359–1368.
18. Boyd, L., Guo, S., Levitan, D., Stinchcomb, D.T., and Kemphues, K.J. (1996). PAR-2 is asymmetrically distributed and promotes association of P granules and PAR-1 with the cortex in C. elegans embryos. Development *122*, 3075–3084.
19. Guo, S., and Kemphues, K.J. (1995). par-1, a gene required for establishing polarity in C. elegans embryos, encodes a putative Ser/Thr kinase that is asymmetrically distributed. Cell *81*, 611–620.
20. Achilleos, A., Wehman, A.M., and Nance, J. (2010). PAR-3 mediates the initial clustering and apical localization of junction and polarity proteins during C. elegans intestinal epithelial cell polarization. Development *137*, 1833–1842.
21. Legouis, R., Gansmuller, A., Sookhareea, S., Bosher, J.M., Baillie, D.L., and Labouesse, M. (2000). LET-413 is a basolateral protein required for the assembly of adherens junctions in Caenorhabditis elegans. Nat. Cell Biol. *2*, 415–422.
22. Chalmers, A.D., Pambos, M., Mason, J., Lang, S., Wylie, C., and Papalopulu, N. (2005). aPKC, Crumbs3 and Lgl2 control apicobasal polarity in early vertebrate development. Development *132*, 977–986.
23. Klezovitch, O., Fernandez, T.E., Tapscott, S.J., and Vasioukhin, V. (2004). Loss of cell polarity causes severe brain dysplasia in Lgl1 knockout mice. Genes Dev. *18*, 559–571.
24. Ohshiro, T., Yagami, T., Zhang, C., and Matsuzaki, F. (2000). Role of cortical tumour-suppressor proteins in asymmetric division of Drosophila neuroblast. Nature *408*, 593–596.
25. Sonawane, M., Carpio, Y., Geisler, R., Schwarz, H., Maischein, H.-M., and Nuesslein-Volhard, C. (2005). Zebrafish penner/lethal giant larvae

2 functions in hemidesmosome formation, maintenance of cellular morphology and growth regulation in the developing basal epidermis. Development *132*, 3255–3265.
26. Betschinger, J., Eisenhaber, F., and Knoblich, J.A. (2005). Phosphorylation-induced autoinhibition regulates the cytoskeletal protein Lethal (2) giant larvae. Curr. Biol. *15*, 276–282.
27. De Lorenzo, C., Strand, D., and Mechler, B.M. (1999). Requirement of Drosophila l(2)gl function for survival of the germline cells and organization of the follicle cells in a columnar epithelium during oogenesis. Int. J. Dev. Biol. *43*, 207–217.
28. Peng, C.Y., Manning, L., Albertson, R., and Doe, C.Q. (2000). The tumour-suppressor genes lgl and dlg regulate basal protein targeting in Drosophila neuroblasts. Nature *408*, 596–600.
29. Brangwynne, C.P., Eckmann, C.R., Courson, D.S., Rybarska, A., Hoege, C., Gharakhani, J., Jülicher, F., and Hyman, A.A. (2009). Germline P granules are liquid droplets that localize by controlled dissolution/condensation. Science *324*, 1729–1732.
30. Cheeks, R.J., Canman, J.C., Gabriel, W.N., Meyer, N., Strome, S., and Goldstein, B. (2004). C. elegans PAR proteins function by mobilizing and stabilizing asymmetrically localized protein complexes. Curr. Biol. *14*, 851–862.
31. Hao, Y., Boyd, L., and Seydoux, G. (2006). Stabilization of cell polarity by the C. elegans RING protein PAR-2. Dev. Cell *10*, 199–208.
32. Hutterer, A., Betschinger, J., Petronczki, M., and Knoblich, J.A. (2004). Sequential roles of Cdc42, Par-6, aPKC, and Lgl in the establishment of epithelial polarity during Drosophila embryogenesis. Dev. Cell *6*, 845–854.
33. Watts, J.L., Etemad-Moghadam, B., Guo, S., Boyd, L., Draper, B.W., Mello, C.C., Priess, J.R., and Kemphues, K.J. (1996). par-6, a gene involved in the establishment of asymmetry in early C. elegans embryos, mediates the asymmetric localization of PAR-3. Development *122*, 3133–3140.
34. Petrásek, Z., Hoege, C., Mashaghi, A., Ohrt, T., Hyman, A.A., and Schwille, P. (2008). Characterization of protein dynamics in asymmetric cell division by scanning fluorescence correlation spectroscopy. Biophys. J. *95*, 5476–5486.
35. Vasioukhin, V. (2006). Lethal giant puzzle of Lgl. Dev. Neurosci. *28*, 13–24.
36. Hannak, E., Kirkham, M., Hyman, A.A., and Oegema, K. (2001). Aurora-A kinase is required for centrosome maturation in Caenorhabditis elegans. J. Cell Biol. *155*, 1109–1116.
37. Brenner, S. (1974). The genetics of Caenorhabditis elegans. Genetics *77*, 71–94.
38. Praitis, V., Casey, E., Collar, D., and Austin, J. (2001). Creation of low-copy integrated transgenic lines in Caenorhabditis elegans. Genetics *157*, 1217–1226.
39. Schonegg, S., Constantinescu, A.T., Hoege, C., and Hyman, A.A. (2007). The Rho GTPase-activating proteins RGA-3 and RGA-4 are required to set the initial size of PAR domains in Caenorhabditis elegans one-cell embryos. Proc. Natl. Acad. Sci. USA *104*, 14976–14981.
40. Munro, E., Nance, J., and Priess, J.R. (2004). Cortical flows powered by asymmetrical contraction transport PAR proteins to establish and maintain anterior-posterior polarity in the early C. elegans embryo. Dev. Cell *7*, 413–424.
41. Kraemer, B., Crittenden, S., Gallegos, M., Moulder, G., Barstead, R., Kimble, J., and Wickens, M. (1999). NANOS-3 and FBF proteins physically interact to control the sperm-oocyte switch in Caenorhabditis elegans. Curr. Biol. *9*, 1009–1018.
42. Kamath, R.S., Martinez-Campos, M., Zipperlen, P., Fraser, A.G., and Ahringer, J. (2001). Effectiveness of specific RNA-mediated interference through ingested double-stranded RNA in Caenorhabditis elegans. Genome Biol. *2*, H0002.
43. Timmons, L., and Fire, A. (1998). Specific interference by ingested dsRNA. Nature *395*, 854.